Advances in Applied Mathematics and Mechanics
Adv. Appl. Math. Mech., Vol. **16**, No. 2, pp. 355-372

DOI: 10.4208/aamm.OA-2021-0148
April 2024

Natural Frequencies of Composite Lattice Structure Surrounded by Winkler–Pasternak Ambient using Galerkin Method

Ehsaneh Mohammadpour Hamedani and Amir H. Hashemian*

Department of Aerospace Engineering, Science and Research Branch, Islamic Azad University, Tehran, Iran

Received 1 May 2021; Accepted (in revised version) 20 February 2022

Abstract. The present work contains an analytical expression and solution for free vibration problem of a composite lattice cylindrical shell surrounded by Winkler–Pasternak elastic foundation with clamped edges. The foundation is simulated using a large number of linear, homogenous shear and radial springs with variable stiffness. An integrated formula for calculation of the natural frequency of lattice structure and its foundation is derived from the equations of motion of the shell implemented by Winkler–Pasternak terms based on Fourier decomposition and Galerkin method. The fundamental frequency formula concerning the foundation elements and lattice parameters is an effective means of estimation frequency in earlier design phase and also a tool to assess the vibration analysis of composite lattice cylindrical shell surrounded by an elastic foundation in design analysis and numerical solutions. The results are verified and confirmed using finite element analysis which show a very good agreement.

AMS subject classifications: 35-11, 35E05

Key words: Free vibrations, elastic foundation Winkler–Pasternak, fundamental frequency, Galerkin's method, composite lattice cylindrical shell.

1 Introduction

Lattice composite structures resting on/or surrounded by elastic foundations, have an outstanding roll in different fields of engineering such as aerospace, mechanics, marine and modern civil structures. Different studies on the natural frequency of beams resting on elastic foundations and analytical solutions for beams subjected to arbitrary dynamic loads have been done, but rare studies about a lattice structure on elastic Winkler–Pasternak foundation could be observed. The natural frequency of finite Timoshenko

*Corresponding author.
Email: ah.hashemian@gmail.com (A. Hashemian)

beams on Pasternak foundations has been analyzed with six cases of bounding conditions [1]. M. K. Ahmed has studied the natural frequencies and mode shapes of a variable thickness elastic cylindrical shell, resting on Pasternak foundation using transfer matrix [2]. D. N. Paliwal and R. Pandey studied the free vibration of an orthotropic thin cylindrical shell on a Pasternak foundation [3]. Morozov et al. obtained a solution for free vibration problem of a composite lattice shell with clamped boundary conditions [4]. They used a continuous model on which, the lattice cylinder has been replaced with a thin orthotropic shell, with the same corresponding structural stiffness. Mozorov et al. [5] and Vasiliev et al. [6, 7] have considered continuous finite element models for anisogrid composite structure, using beam, shell or solid elements. An Hou et al. examined the failure modes of both cylindrical and conical composite lattice shells. They compared the numerical results obtained by finite element analysis with experimental solutions [8]. G. Totaro analyzed the local buckling failure modes for composite anisogrid lattice cylindrical shells with a typical system of hexagonal cells. The local buckling of helical ribs is normally based on a simplified and qualitative approach, based on Ritz method. This model has been verified with the aid of finite-element analysis, demonstrating a noteworthy accuracy [9]. Xu et al. investigated the natural frequencies of composite sandwich beams with lattice truss core, by combining the Euler-Bernoulli and Timoshenko beam theories. They derived the governing partial differential equations of motion, using Hamilton's principle and obtained an analytical formulation for determining the natural frequencies [10]. Frulloni et al. studied the behavior of lattice composite hollow structures that have been subjected to an external hydrostatic pressure, using finite element modeling [11]. Jeon et al. introduced the critical stress function utilized in failure criterion, from the compression test results. The finite element analysis was used to calculate the failure load with the proposed failure criterion and also the buckling load for the full-sized cylindrical lattice structures [12]. Kim et al. applied composite lattice rectangular plates for the solar panels of a high-agility satellite. They proposed an approximate method of conducting vibration, buckling analyses of the lattice plate of the solar panel with a torsional spring using the Ritz method. This method considers the buckling as well as the vibration characteristics (natural frequencies and modes). The validity was verified by comparing the results with finite-element analysis [13]. Most recent researches have been focused on failure, design, buckling and vibrations of lattice structures due to different loads and conditions, but the influence of the foundations is not considered in most of these studies. The aim of the present study is to obtain an analytical expression for natural frequencies of lattice cylindrical shells, composed of helical and radial ribs, surrounded by an elastic Winkler–Pasternak foundation. By solving the governing equation using Galerkin method, an analytical compact expression can be obtained in order to make the possibility of tuning design parameters, to reach the design goal without consumption and utilization of cost and time for numerical modeling and modal analysis. Also, the effect of the shell's length and stiffness of shearing and radial springs on natural frequencies and stability of the cylindrical lattice shell are investigated.

2 Governing equations, theory and mathematical model

A classical theory and modeling of elastic foundation in the radial direction has been used to derive the governing equations of natural frequencies of a lattice cylindrical shell. In order to have a clear inspection for the foundation model and governing equations of motion of the lattice cylindrical shell, each are discussed separately.

2.1 Foundation model

The composite lattice cylindrical structure is considered to be shrouded from its outer side by a linear, homogenous and elastic foundation in axial direction. The Winkler–Pasternak foundation can be assumed as radial and shear layer springs with two stiffness coefficients of K and G, in longitudinal axes. The springs are assumed to have pure displacement, they are fully independent, with no integration and coupling effect with each other. The simple and normal response of the foundation to load $p(x,y)$ can be written as;

$$p(x,y)=Kw-G\nabla^2 w, \tag{2.1}$$

in which w is the displacement along y axis and ∇^2 is the Laplace operator;

$$\nabla^2=\frac{\partial^2}{\partial\alpha^2}+\frac{1}{R^2}\frac{\partial^2}{\partial\beta^2}. \tag{2.2}$$

Figs. 1(a) and (b) show the coordinate axes, α, β and γ of the cylindrical shell, with radius R and length L and a schematic of an elastic Winkler–Pasternak foundation, respectively.

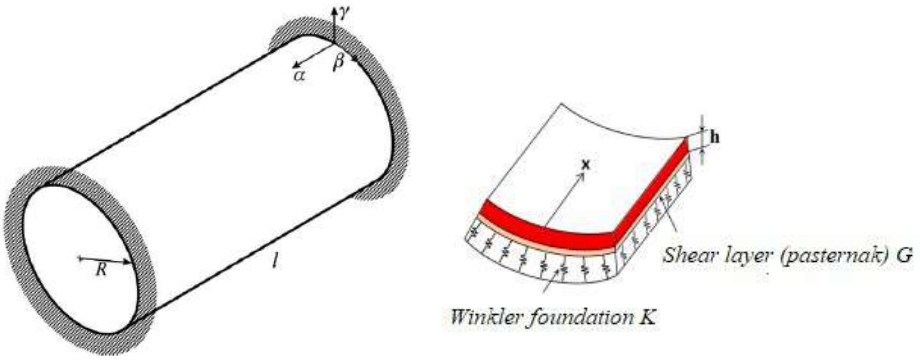

(a) (b)

Figure 1: (a) Coordinate axes of the cylindrical shell [3]; (b) Schematic of elastic Winkler–Pasternak foundation.

2.2 Governing equations

The lattice cylindrical shell consists of helical and hoop ribs which pass through the midpoints of the helical segments as it is shown in Fig. 2. Geometrical parameters can be calculated from the continuum model of the lattice cylindrical shell as shown in Fig. 2. The structure is characterized by the rib height h, angle of orientation ϕ of the helical ribs, a_s and a_r are the distances between the helical and hoop ribs, respectively. n_s is the number of helical ribs of one direction and δ_s and δ_r are the width of helical and hoop ribs, respectively. Also E_s, E_r, ρ_s and ρ_r are the modulus of elasticity and density of helical and hoop ribs' material, respectively. The mass per unit area of the shell surface is shown as B_ρ. The following equations are used to calculate the lattice cylinder parameters [4]:

$$a_s=\frac{2\pi R}{n_s}\cos\phi,\qquad a_r=\frac{\pi R}{n_s tg\phi},\quad f_{11}=\frac{\cos^3\phi}{\pi}, \tag{2.3a}$$

$$f_{12}=\frac{\cos\phi\sin^2\phi}{\pi},\quad f_{22}=\frac{\sin\phi}{\pi\cos\phi}\left(\sin^3\phi+\frac{E_r}{E_s}\frac{\sigma_r}{\sigma_s}\right),\quad f_p=\frac{1}{\pi\cos\phi}\left(1+\frac{\rho_r}{\rho_s}\frac{\delta_r}{\delta_s}\sin\phi\right), \tag{2.3b}$$

$$A_{11}=2E_S\frac{\delta_S}{a_s}\cos^4\phi,\quad A_{12}=A_{33}=2E_S\frac{\sigma_S}{a_s}\cos^2\phi\sin^2\phi,\quad A_{22}=2E_S\frac{\sigma_s}{a_s}\sin^4\phi+E_r\frac{\sigma_r}{a_r}, \tag{2.3c}$$

$$A_\rho=2\rho_s\frac{\delta_s}{a_s}+\rho_r\frac{\delta_r}{a_r},\quad B_{11}=A_{11}h,\quad B_{12}=A_{12}h,\quad B_{22}=A_{22}h,\quad B_{33}=A_{33}h, \tag{2.3d}$$

$$B_p=A_\rho h,\quad D_{11}=A_{11}\frac{h^3}{12},\quad D_{12}=A_{12}\frac{h^3}{12},\quad D_{22}=A_{22}\frac{h3}{12},\quad D_{33}=A_{33}\frac{h^3}{12}. \tag{2.3e}$$

The equation of motion is derived, using the classical theory of orthotropic cylindrical shells [3]. The first approach makes use of continuum models that employ various modifications of rib smearing techniques. In this case, the lattice structure is modeled as a shell having the averaged (smeared) stiffness. The corresponding stiffness coefficients are calculated using the rib smearing techniques and depend on the number and orientation of the ribs and their stiffness. The models are analyzed using conventional theories of the continuum orthotropic shells. For applying the continuous model of shell, adequate number of helical and hoop ribs are used for the lattice structure to reach the defined density. The lattice composite cylindrical structure is replaced with a continuous orthotropic

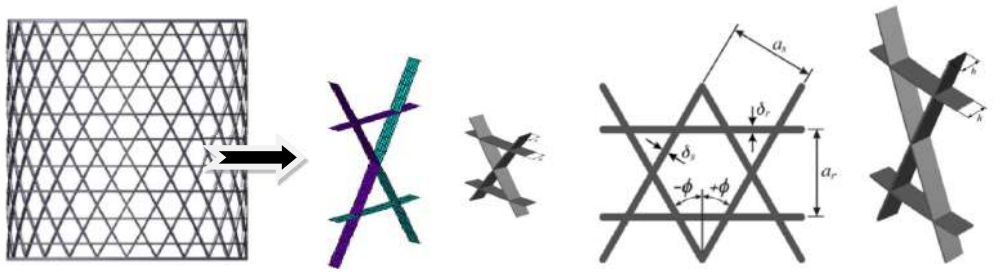

Figure 2: Lattice cylindrical shell composed of helical and hoop ribs [3].

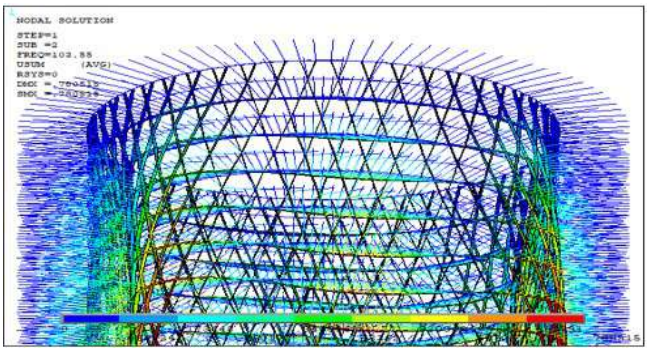

Figure 3: The lattice shell surrounded by elastic foundation.

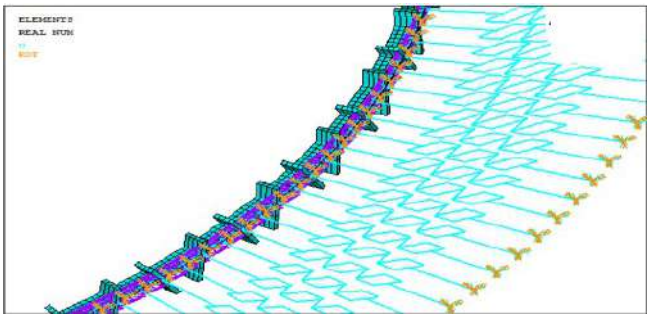

Figure 4: The elastic foundation is modeled as radial springs.

shell, having equivalent effective stiffness [4]. Also the composite lattice structure is assumed to be unidirectional which simplifies the equations. The equation of motion in cylindrical coordinate is given as,

$$\frac{\partial N_\alpha}{\partial \alpha}+\frac{\partial N_{\alpha\beta}}{\partial \beta}-\beta_\rho \frac{\partial^2 u}{\partial t^2}=0, \tag{2.4a}$$

$$\frac{\partial N_{\alpha\beta}}{\partial \alpha}+\frac{\partial N_\beta}{\partial \beta}+\frac{1}{R}\frac{M_{\alpha\beta}}{\partial \beta}+\frac{1}{R}\frac{M_\beta}{\partial \beta}-\beta_\rho \frac{\partial^2 v}{\partial t^2}=0, \tag{2.4b}$$

$$\frac{\partial^2 M_\alpha}{\partial \alpha^2}+\frac{2\partial^2 M_{\alpha\beta}}{\partial \alpha \partial \beta}+\frac{\partial^2 M_\beta}{\partial \beta^2}-\frac{N_\beta}{R}-\beta_\rho \frac{\partial^2 w}{\partial t^2}=0. \tag{2.4c}$$

In which β_ρ is the mass of the shell per unit area. Also, N_α, N_β, $N_{\alpha\beta}$ and M_α, M_β, $M_{\alpha\beta}$ are the components of stress resultant and the bending and twisting moments, respectively. The displacements u, v and w are the displacements along α, β and γ axes, respectively. The term for elastic Winkler–Pasternak foundation can be applied to the right side of third equation of Eq. (2.4), to obtain Eq. (2.5). Figs. 3 and 4 show the radial springs as an

elastic ambient, limiting the outer surface of the lattice structure

$$\frac{\partial N_\alpha}{\partial \alpha}+\frac{\partial N_{\alpha\beta}}{\partial \beta}-B_\rho\frac{\partial^2 u}{\partial t^2}=0, \tag{2.5a}$$

$$\frac{\partial N_{\alpha\beta}}{\partial \alpha}+\frac{\partial N_\beta}{\partial \beta}+\frac{1}{R}\frac{M_{\alpha\beta}}{\partial \beta}+\frac{1}{R}\frac{M_\beta}{\partial \beta}-B_\rho\frac{\partial^2 v}{\partial t^2}=0, \tag{2.5b}$$

$$\frac{\partial^2 M_\alpha}{\partial \alpha^2}+\frac{\partial^2 M_{\alpha\beta}}{\partial \alpha\partial \beta}+\frac{\partial^2 M_\beta}{\partial \beta^2}-\frac{N_\beta}{R}-B_\rho\frac{\partial^2 w}{\partial t^2}=Kw-G\nabla^2 w. \tag{2.5c}$$

The terms of Eq. (2.5) should be complemented by establishing equations for orthotropic and quasi-orthotropic composite materials which are derived from Eq. (2.6)

$$\begin{bmatrix} N_\alpha \\ N_\beta \\ N_{\alpha\beta}\end{bmatrix}=\begin{bmatrix} B_{11} & B_{12} & 0 \\ B_{21} & B_{22} & 0 \\ 0 & 0 & B_{33}\end{bmatrix}\begin{bmatrix} \varepsilon_\alpha \\ \varepsilon_\beta \\ \varepsilon_{\alpha\beta}\end{bmatrix}, \tag{2.6a}$$

$$\begin{bmatrix} M_\alpha \\ M_\beta \\ M_{\alpha\beta}\end{bmatrix}=\begin{bmatrix} D_{11} & D_{12} & 0 \\ D_{21} & D_{22} & 0 \\ 0 & 0 & D_{33}\end{bmatrix}\begin{bmatrix} \kappa_\alpha \\ \kappa_\beta \\ \kappa_{\alpha\beta}\end{bmatrix}. \tag{2.6b}$$

Where B_{11}, B_{12}, B_{22}, B_{33}, ($B_{12}=B_{21}$) and D_{11}, D_{12}, D_{22}, D_{33}, ($D_{12}=D_{21}$) are the membrane strains of the middle surface. κ_α, κ_β and $\kappa_\alpha\beta$ are curvature and deformation of middle surface and ε_α, ε_β and $\varepsilon_\alpha\beta$ are the displacement relations, given by:

$$\varepsilon_\alpha=\frac{\partial u}{\partial \alpha},\qquad \varepsilon_\beta=\frac{\partial u}{\partial \beta}+\frac{W}{R},\qquad \varepsilon_{\alpha\beta}=\frac{\partial u}{\partial \beta}+\frac{\partial v}{\partial \alpha}, \tag{2.7a}$$

$$\kappa_\alpha=-\frac{\partial^2 w}{\partial \alpha^2},\qquad \kappa_\beta=-\frac{\partial^2 w}{\partial \beta^2}+\frac{1}{R}\frac{\partial v}{\partial \beta},\qquad \kappa_{\alpha\beta}=-2\frac{\partial^2 w}{\partial \alpha\partial \beta}+\frac{1}{R}\frac{\partial v}{\partial \alpha}, \tag{2.7b}$$

u and v are axial and circumferential displacements of the middle surface and w is the shell deflection. Four boundary conditions are needed as

$$u=0,\quad \nu=0,\quad \omega=0,\quad \frac{\partial w}{\partial \alpha}=0.$$

By substituting Eqs. (2.6) and (2.7) into Eq. (2.5), a generalized governing equation of motion can be obtained, considering the elastic properties of the Winkler–Pasternak foundation as the third term of Eq. (2.8)

$$B_{11}\frac{\partial^2 u}{\partial \alpha^2}+B_{33}\frac{\partial^2 u}{\partial \beta^2}+(B_{12}+B_{33})\frac{\partial^2 v}{\partial \alpha\partial \beta}+\frac{B_{12}}{R}\frac{\partial w}{\partial \alpha}-B_\rho\frac{\partial^2 u}{\partial t^2}=0, \tag{2.8a}$$

$$(B_{12}+B_{33})\frac{\partial^2 u}{\partial\alpha\partial\beta}+\left(B_{33}+\frac{D_{33}}{R^2}\right)\frac{\partial^2 v}{\partial\alpha^2}+\left(B_{22}+\frac{D_{22}}{R_2}\right)\frac{\partial^2 v}{\partial\beta^2}+\frac{B_{22}}{R}\frac{\partial w}{\partial\beta}$$
$$-\frac{D_{12}+2D_{33}}{R}\frac{\partial^3 w}{\partial\alpha^2\partial\beta}-\frac{D_{22}}{R}\frac{\partial^3\omega}{\partial\beta^3}-B_\rho\frac{\partial^2 v}{\partial t^2}=0, \tag{2.8b}$$
$$-\frac{B_{12}}{R}\frac{\partial u}{\partial\alpha}-\frac{B_{22}}{R}\frac{\partial v}{\partial\beta}+\frac{D_{22}}{R}\frac{\partial^3 v}{\partial\beta^3}+\frac{D_{12}+2D_{33}}{R}\frac{\partial^3 v}{\partial\alpha^2\partial\beta}-\frac{B_{22}}{R^2}w-D_{11}\frac{\partial^4 w}{\partial\alpha^4}$$
$$-2(D_{12}+2D_{33})\frac{\partial^4 w}{\partial\alpha^2\partial\beta^2}-D_{22}\frac{\partial^4 w}{\partial\beta^4}-Kw+G\frac{\partial^2 w}{\partial\alpha^2}+\frac{G}{R^2}\frac{\partial^2 w}{\partial\beta^2}+B_\rho\omega^2 w=0. \tag{2.8c}$$

Where K and G are the Winker and Pasternak coefficients, respectively.

3 Solution method

In order to solve the third term of Eq. (2.8) analytically, the shell displacements u, v and w, can be presented as:

$$\begin{cases} u(\alpha,\beta,t)=u(\alpha,\beta)\cos\omega t, \\ v(\alpha,\beta,t)=v(\alpha,\beta)\cos\omega t, \\ w(\alpha,\beta,t)=w(\alpha,\beta)\cos\omega t. \end{cases} \tag{3.1}$$

By substituting Eq. (3.1) into Eq. (2.8), Eq. (3.2) is derived

$$B_{11}\frac{\partial^2 u}{\partial\alpha^2}+B_{33}\frac{\partial^2 u}{\partial\beta^2}+(B_{12}+B_{33})\frac{\partial^2 v}{\partial\alpha\partial\beta}+\frac{B_{12}}{R}\frac{\partial w}{\partial\alpha}+B_\rho\omega^2 u=0, \tag{3.2a}$$
$$(B_{12}+B_{33})\frac{\partial^2 u}{\partial\alpha\partial\beta}\left(B_{33}+\frac{D_{33}}{R^2}\right)\frac{\partial^2 v}{\partial\alpha^2}+\left(B_{22}+\frac{D_{22}}{R^2}\right)\frac{\partial^2 v}{\partial\beta^2}+\frac{B_{22}}{R}\frac{\partial w}{\partial\beta}$$
$$-\frac{D_{12}+2D_{33}}{R}+\frac{\partial^3 w}{\partial\alpha^2\partial\beta}-\frac{D_{22}}{R}\frac{\partial^3 w}{\partial\beta^3}+B_\rho\omega^2 v=0, \tag{3.2b}$$
$$-\frac{B_{12}}{R}\frac{\partial u}{\partial\alpha}-\frac{B_{22}}{R}\frac{\partial v}{\partial\beta}+\frac{D_{22}}{R}\frac{\partial^3 v}{\partial\beta^3}+\frac{D_{12}+2D_{33}}{R}\frac{\partial^3 v}{\partial\alpha^2\partial\beta}-\frac{B_{22}}{R^2}w-D_{11}\frac{\partial^4 w}{\partial\alpha^4}-2(D_{12}+2D_{33})\frac{\partial^4\omega}{\partial\alpha^2\partial\beta^2}$$
$$-D_{22}\frac{\partial^4\omega}{\partial\beta^4}+B_\rho\omega_n^2 w-Kw+G\frac{\partial^2}{\partial\alpha^2}(\omega\cos\omega t)+\frac{G}{R^2}\frac{\partial^2}{\partial\beta^2}(\omega\cos\omega t)=0. \tag{3.2c}$$

By solving the above equations along with their homogenous boundary values, the fundamental frequency for the lattice cylindrical shell can be obtained. Trigonometry series as in Eq. (3.3) can be employed to be expanded along hoop coordinate β, because the reflecting deformation function of the circular cylindrical shell is periodical

$$u(\alpha,\beta)=\sum_{n=1}^{\infty}u_n(\alpha)\cos\lambda_n\beta, \tag{3.3a}$$

$$v(\alpha,\beta)=\sum_{n=1}^{\infty}v_n(\alpha)\sin\lambda_n\beta, \tag{3.3b}$$

$$w(\alpha,\beta)=\sum_{n=1}^{\infty}w_n(\alpha)\cos\lambda_n\beta. \tag{3.3c}$$

Substituting Eq. (3.3) to (3.2), the following homogenous system of ordinary equations is derived

$$B_{11}\frac{\partial^2 u_n}{\partial\alpha^2}-B_{33}{\lambda_n}^2u_n+(B_{12}+B_{33})\lambda_n\frac{\partial v_n}{\partial\alpha}+\frac{B_{12}}{R}\frac{\partial w_n}{\partial\alpha}+B_\rho\omega_n^2u_n=0, \tag{3.4a}$$

$$-(B_{12}+B_{33})\lambda_n\frac{\partial u_n}{\partial\alpha}+\left(B_{33}+\frac{D_{33}}{R^2}\right)\frac{\partial^2 v_n}{\partial\alpha^2}-\left(B_{22}+\frac{D_{22}}{R^2}\right)\lambda_n^2v_n+\frac{D_{12}+2D_{33}}{R}\lambda_n\frac{\partial^2 w_n}{\partial\alpha^2}$$
$$-\frac{\lambda_n}{R}\left(B_{12}+D_{22}{\lambda_n}^2\right)w_n+B_\rho\omega_n^2v_n=0, \tag{3.4b}$$

$$\frac{B_{12}}{R}\frac{\partial u_n}{\partial\alpha}-\frac{\lambda_n}{R}\left(B_{22}+D_{22}\lambda_n^2\right)v_n+\frac{D_{12}+2D_{33}}{R}\lambda_n\frac{d^2v_n}{d\alpha^2}-\left(\frac{B_{22}}{R^2}+D_{22}\lambda_n^4\right)w_n-D_{11}\frac{\partial^4 w_n}{\partial\alpha^4}$$
$$+2(D_{12}+2D_{33})\lambda_n^2\frac{\partial^2 w_n}{\partial\alpha^2}-Kw+G\frac{\partial^2 w_n}{\partial\alpha^2}-\frac{1}{R^2}Gw_n\lambda_n^2+B_\rho\omega_n^2w_n=0. \tag{3.4c}$$

In which ω_n is the nth harmonic natural frequency. The new boundary conditions adopted by Eq. (3.4) are

$$u_n=0,\quad v_n=0,\quad w_n=0,\quad \frac{dw_n}{d\alpha}=0. \tag{3.5}$$

The Galerkin method has been used to solve the third term of homogeneous boundary-value problem in Eq. (3.4). So a rapid and good approximating function should be employed to satisfy the boundary conditions of Eq. (3.5). The clamped-clamped boundary conditions are assumed in order to generate the fundamental modes of vibrations of the cylindrical shell, by using the approximated functions. A good approximation for $u_n(\alpha)$, $v_n(\alpha)$ and $w_n(\alpha)$ is represented as follows

$$u_n=U_n\frac{dX}{d\alpha},\quad v_n=V_nX,\quad w_n=W_nX. \tag{3.6}$$

Where

$$X=\cosh\frac{\lambda\alpha}{L}-\cos\frac{\lambda\alpha}{L}-\sigma\left(\sinh\frac{\lambda\alpha}{L}-\sin\frac{\lambda\alpha}{L}\right).$$

In the above equation, λ and σ are constant values. According to the Galerkin method, the expressions for the errors are given by:

$$Z_\alpha = \left(B_{11}\frac{d^3X}{d\alpha^3} - B_{33}\lambda_n^2\frac{dX}{d\alpha}\right)U_n + (B_{12}+B_{33})\lambda_n V_n\frac{dX}{d\alpha} + \frac{B_{12}}{R}\frac{dX}{d\alpha}W_n + B\rho\omega_n^2\frac{dX}{d\alpha}U_n, \quad (3.7a)$$

$$Z_B = -(B_{12}+B_{33})\lambda_n U_n\frac{d^2X}{d\alpha^2} + \left[\left(B_{33}+\frac{D_{33}}{R^2}\right)\frac{d^2X}{d\alpha^2} - \left(B_{22}+\frac{D_{22}}{R^2}\right)\lambda_n^2 X\right]V_n + \lambda_n\left(\frac{D_{12}+2D_{33}}{R}\frac{d^2X}{d\alpha^2} - \frac{B_{22}+D_{22}\lambda_n^2}{R}X\right)W_n + B_\rho\omega_n^2 X V_n, \quad (3.7b)$$

$$Z_\gamma = \frac{-B_{12}}{R}\left[\frac{d}{d\alpha}U_n\frac{dX}{d\alpha}\right] - \frac{\lambda_n}{R}\left(B_{22}+D_{22}\lambda_n^2\right)V_n X + \frac{D_{12}+2D_{33}}{R}\lambda_n\frac{d^2}{d\alpha^2}[V_n X] - \left(\frac{B_{22}}{R^2}+D_{22}\lambda_n^4\right)W_n X - D_{11}\frac{d^4}{d\alpha^4}(W_n X) + 2(D_{12}+2D_{33})\lambda_n^2\frac{d^2}{d\alpha^2}(W_n X) + B_\rho\omega_n^2 W_n X - KW_n X + G\frac{d^2}{d\alpha^2}(W_n X) - \frac{1}{R^2}G\lambda_n^2 W_n X. \quad (3.7c)$$

The unknown constants U_n, V_n and W_n could be found from Eq. (3.7), then the suitable approximated function X and $\frac{dX}{d\alpha}$ could be obtained. Using Galerkin's method gives the following terms:

$$\int_0^L z_\alpha\frac{dX}{d\alpha}d\alpha = 0, \quad \int_0^L z_\beta X d\alpha = 0, \quad \int_0^L z_\gamma X d\alpha = 0. \quad (3.8)$$

Substituting Eq. (3.7) into (3.8) and assuming $\xi = \sigma\lambda(\sigma\lambda - 2)$, the third term of Eq. (3.4) could be derived after some mathematical rearrangement

$$-B_{12}\overline{U}_n\xi + n\left[\left(B_{22}+\frac{D_{22}}{R^2}n^2\right)s + \left(\frac{D_{12}+2D_{33}}{R^2}\frac{\xi}{s}\right)\right]V_n + \left[\left(B_{22}+D_{22}\frac{n^4}{R^2}+\frac{D_{11}}{R^2}\frac{\lambda^4}{s^4}\right) + 2\left(\frac{D_{12}+2D_{33}}{R^2}\right)n^2\frac{\xi}{s} + G\frac{\xi}{s} + \left(K+G\frac{n^2}{R^4}\right)sR^2\right]W_n - \omega_n^2 B_\rho RLW_n = 0. \quad (3.9)$$

Where $\bar{U}_n = \frac{U_n}{L}$, $s = \frac{L}{R}$.

By using the parameters which are defined in the Eq. (2.3) and appendix and substituting into Eq. (3.9) and dividing the resultant equation by $E_s\sigma_s n_s\frac{h}{R}$, the subsequent equation will be derived

$$-\frac{E}{s}\frac{\sigma_s}{R}n_s f_{12}h\overline{U}_n\xi + n\left[\left(E_s\frac{\sigma_s}{R}n_s f_{12}h + \frac{h^3}{12}E_s\frac{\sigma_s}{R}n_s f_{12}\right)s + \frac{1}{R^2}\left(\frac{h^2}{12}E_s\frac{\sigma_s}{R}n + f_{12} + \frac{2h^3}{12}E_s\frac{\sigma_s}{R}n_s f_{12}\right)n^2\frac{\xi}{s}\right]V_n$$

$$+\left[nt_s\frac{\sigma_s}{R}n_sf_{22}+\frac{h^3}{12}E_s\frac{\sigma_s}{R}n_sf_{22}\frac{n^4}{R^2}+\frac{h^3}{12R^2}\frac{\lambda^4}{s^4}n_sf_n+\frac{2}{R^2}\left(\frac{h^3}{R}E_s\frac{\sigma_s}{R}n_sf_{12}+2\frac{h^3}{12}E_s\right)\right.$$
$$\left.+\frac{1}{R^2}G\frac{\xi}{s}+\left(K+\frac{1}{R^2}G\frac{n^2}{R^2}\right)sR^2\right]W_n-\omega_n^2h\delta\frac{\sigma_s}{R}n_s\rho_pRLW_n=0. \tag{3.10}$$

The dimensionless frequency parameter could be stated as:

$$\eta_n=\omega_n^2\frac{\rho_s}{E_s}Rl. \tag{3.11}$$

By ignoring the displacement in α direction in comparison with deflection in hoop direction, then the bellow compact equation could be obtained

$$\begin{cases}(c_{11}-\eta_ng_{11})V_n+c_{12}W_n=0,\\ c_{21}V_n+(c_{22}-\eta_ng_{22}+p_{ss})W_n=0.\end{cases} \tag{3.12}$$

The parameters of Eq. (3.12) have been given as the equations in the Appendix. Setting the determinant of the system of equations to zero:

$$\det\begin{vmatrix}c_{11}-\eta_ng_{11} & c_{12}\\ c_{21} & c_{22}-\eta_nG_{22}+P_{ss}\end{vmatrix}=0 \;\Rightarrow\; a\eta_n^2-b\eta_n+c=0, \tag{3.13}$$

yields to:

$$\eta_n=\frac{b-\sqrt{b^2-4ac}}{2a}, \tag{3.14}$$

where

$$a=g_{11}q_{22},\quad b=c_{11}g_{22}+c_{22g}+P_{ss}g_{11}\quad\text{and}\quad c=c_{n1c}c_{22}-{c_{12}}^2+c_{11}P_{ss}. \tag{3.15}$$

The nth frequency ω_n due to η_n is given by:

$$\omega_n=\xi_n\sqrt{\frac{E_s}{\rho_sRl}}. \tag{3.16}$$

The obtained analytical formula as a rapid tool for reliable estimation of fundamental frequency of lattice cylindrical shell surrounded by elastic foundation, will assist in earlier design phase to calculate the natural frequency avoiding time consuming finite element analysis.

4 Numerical solutions and verification

In finite element modeling, a combined 3D element was considered for the lattice structure and shear layer for Winkler parameter (in the direction of cylinder cross section

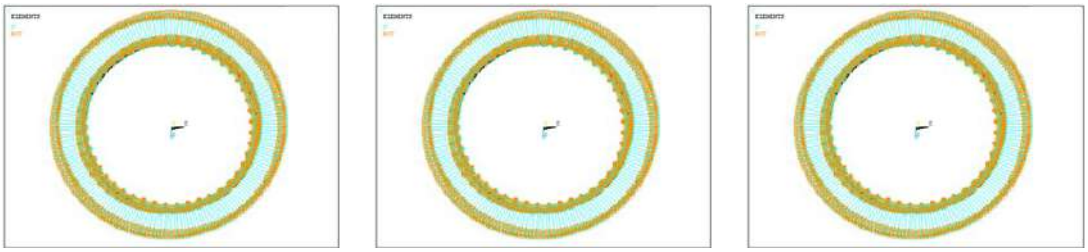

Figure 5: Lattice cylindrical shell surrounded by elastic foundation.

radius). The combined element has 3D applications, pure transfer and no coupling. It has been assumed that the elements have no rotational degree of freedom. Also, the spring element was considered to have no mass. In the first step of modeling the anisogrid structure, simplifications were considered by modeling the smallest reputable cell of the lattice and repeat the result along the axes to have a cylindrical lattice structure with defined R and L as radius and length, respectively. All the keypoints have been merged with defined tolerance to model the integrated structure. For foundation modeling, a proper number of spring elements along $R+H$ (which describes the distance from the outer surface of shell in radial direction) and longitudinal spring elements (with the same location) have been employed as Winkler parameter and Pasternak modules, respectively. Fig. 5 shows the foundation simulation using spring elements with one end attached to the structure, while the other ends are clamped. The geometric parameters of such structures are defined in Table 1.

Before calculating the natural frequencies of the lattice structure located in an ambient of elastic foundation, an analytical calculation has been performed to validate the equation, through a comparison of the natural frequencies of the lattice shell, without the elastic foundation with previous studies. Adding an ambient of elastic foundation, a new analytical formula has been obtained. The results indicated that by employing the elastic foundation, the coefficients of Pasternak and Winkler modulus have an extreme effect on increasing the natural frequencies of the lattice structure. As shown in the results of Table 2, by increasing the number of helical ribs specifically more than 48, and in the presence of the foundation, the natural frequencies will increase. The results in Table 2, were obtained by deriving the governing equations with boundary conditions, using Galerkin method, with and without the elastic ambient and are in good agreement with FEM. The natural frequencies without the elastic foundation have been calculated using the analytic formula for each individual rib's angle and number of helical ribs and were compared with the results of A. V. Lopatin et al. [4]. Then the natural frequencies for each individual rib's angle and number of helical ribs were calculated using the analytic formula for the lattice cylinder with the ambient elastic foundation and were compared with FEM solution. Acceptable results have been achieved and it was observed that the natural frequency has been decreased in different configurations while the elastic foundation

Table 1: Parameters and values of lattice structure.

Parameters	Definition	Value
ρ	Density	1550kg/m^3
E	Module of Elasticity	70*10^{9}N/m^2
R	Lattice Cross section Radius	0.5m
L	Effective lattice length	2m
δ_s	Helical Ribs Thickness	2mm
δ_r	Hoop Ribs Thickness	2mm
ρ_s	Helical Ribs Density	1550kg/m^3
ρ_r	Hoop Ribs Density	1550kg/m^3
H	Ribs Height	8mm
L/R	Length to Radius Ratio	4
R/H	Radius to Ribs Height Ratio	62
P	Poison Ratio	0.32
Φ	Angle between Helical ribs	15°
n_s	Number of Helical Ribs	48
K	Pasternak Coefficient	0, 10 , 10^2 , 10^3, 10^4, 10^5
G	Winkler Coefficient	0,10, 25, 50, 75, 100, 500

Table 2: Natural frequencies from analytic formula with and without elastic foundation for $L=2$m.

Freq. Without Foundation						
n_s	48		60		72	
Ribs Angle	Analytical Solution	Ref. [4]	Analytical Solution	Ref. [4]	Analytical Solution	Ref. [4]
15	103.55	104.37	104.9	104.96	105.7	105.64
20	117.79	115.83	117.07	117.1	117.86	118.52
25	121.89	122.96	124.12	123.11	125.17	124.91
30	122.65	124.92	125.81	125.09	126.9	127.19
35	122.76	123.73	125.82	125.08	126.97	127.17
40	122.39	123.17	125.13	124.8	125.66	126.39
45	110.61	117.83	112.1	118.62	113.43	119.1
Freq. With Elastic Foundation						
n_s	48		60		72	
Ribs Angle	Analytical Solution	FEM	Analytical Solution	FEM	Analytical Solution	FEM
15	100.86	103.01	109.01	113.22	108.97	112.24
20	100.86	103.55	121.68	126.83	121.65	124.80
25	100.87	103.55	127.99	130.32	127.97	132.35
30	100.98	103.56	130.12	133.35	130.10	134.04
35	102.05	103.73	129.97	136.05	129.95	131.02
40	112.19	105.37	129.06	119.16	129.04	118.36
45	112.20	105.98	120.79	117.17	120.78	115.74

is applied.

Fig. 6 shows that the results of analytical solutions are in good agreement with the results of [4], for the lattice structure without elastic foundation. It also shows that the results of analytical solutions are in good agreement with FEM in the presence of elastic foundation.

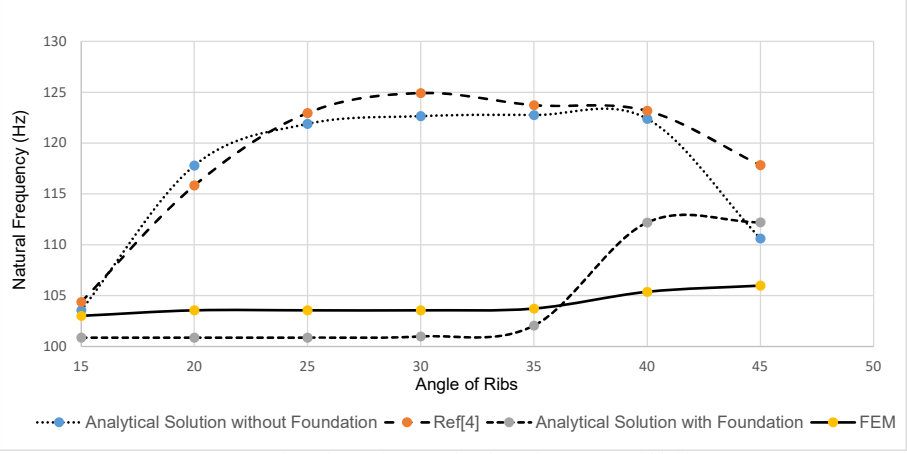

Figure 6: Comparison of natural frequencies of a lattice structure with/without Winkler–Pasternak Foundation with $n_s = 48$.

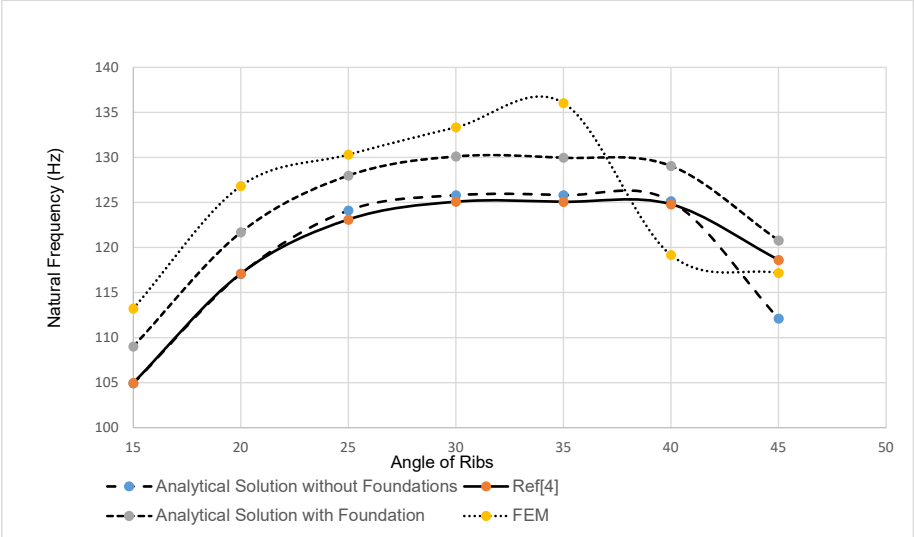

Figure 7: Comparison of natural frequencies of a lattice structure with/without Winkler–Pasternak Foundation with $n_s = 60$.

In Figs. 6-8 the values of natural frequencies for different rib numbers and angles are illustrated. It is shown that the natural frequencies decrease without the elastic foundation. To study the effect of foundation coefficients, K and G, the natural frequencies of the structure, were calculated using Eq. (3.16). Because the modal analysis takes much time with enormous elements within the length of 4 meters and circumferential ribs of 60 and 72, so the calculations were performed for a length of 2 meters and rib angles of

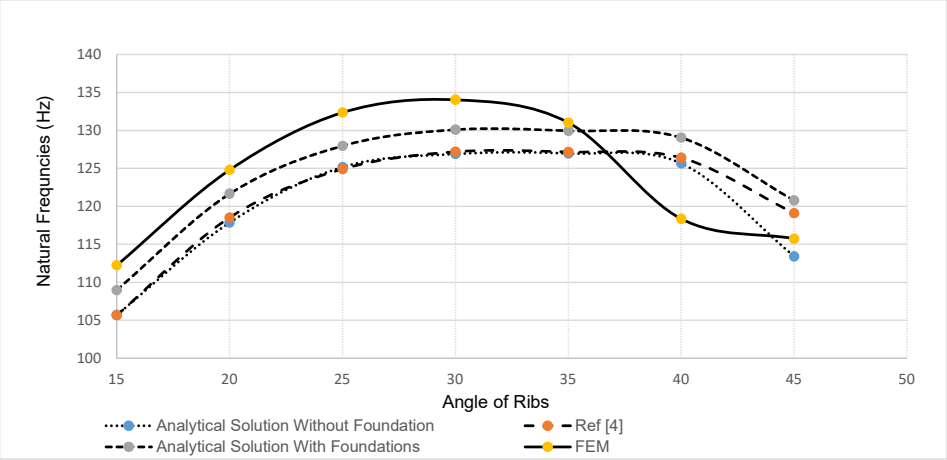

Figure 8: Comparison of natural frequencies of a lattice structure with/without Winkler–Pasternak Foundation with $n_s=72$.

15 degrees. For calculating the natural frequencies for cylinders with other lengths and angles, with different numbers of circumferential ribs, advanced computers with parallel processors are needed. In Fig. 6, in the absence of foundation, the natural frequency increases from rib angle's 15° to 30° and then gradually starts to decrease. By adding the Winkler–Pasternak foundation to the lattice structure, a smooth increase of natural frequency can be observed. In Fig. 7 and also in Fig. 8, the natural frequencies increase from rib angle's 15° to 35° for both cases with and without foundation, but from 35° to 45° the amount of natural frequencies decreases smoothly. However, changing the number of ribs used in lattice structures, causes the variation of natural frequencies. Table 3 shows the variations of Winkler and Pasternak coefficients and their influences on natural frequencies. The stiffness of the structure is affected by two coefficients and each one plays an important role in variation of natural frequencies. As mentioned in Table 3, increasing K, for the elastic foundation while keeping G constant, (and vice versa) will increase the natural frequencies because of increasing the stiffness of the structure proportionally. By applying different values of (K,G), it is observed that the K values are more effective than G values in calculation of natural frequencies.

The finite element model has been applied for the lattice cylindrical shell with 97830 nodes and 3984 springs' elements. The total stiffness follows the rules of parallel springs and is divided by the number of springs, implemented in modeling. A typical fundamental vibration of cylindrical lattice shell surrounded by elastic foundation with clamped edges is analyzed in FEM software. Four mode shapes are shown in Figs. 9 and 10 for $k=100$ and $G=0\text{N/m}^3$. The even shape modes are not shown due to their similarity with odd modes which explains that the clamped lattice structure has longitudinal stability.

Variations of the elastic foundation Winkler coefficient, K, from 0 to 2×10^6 and its

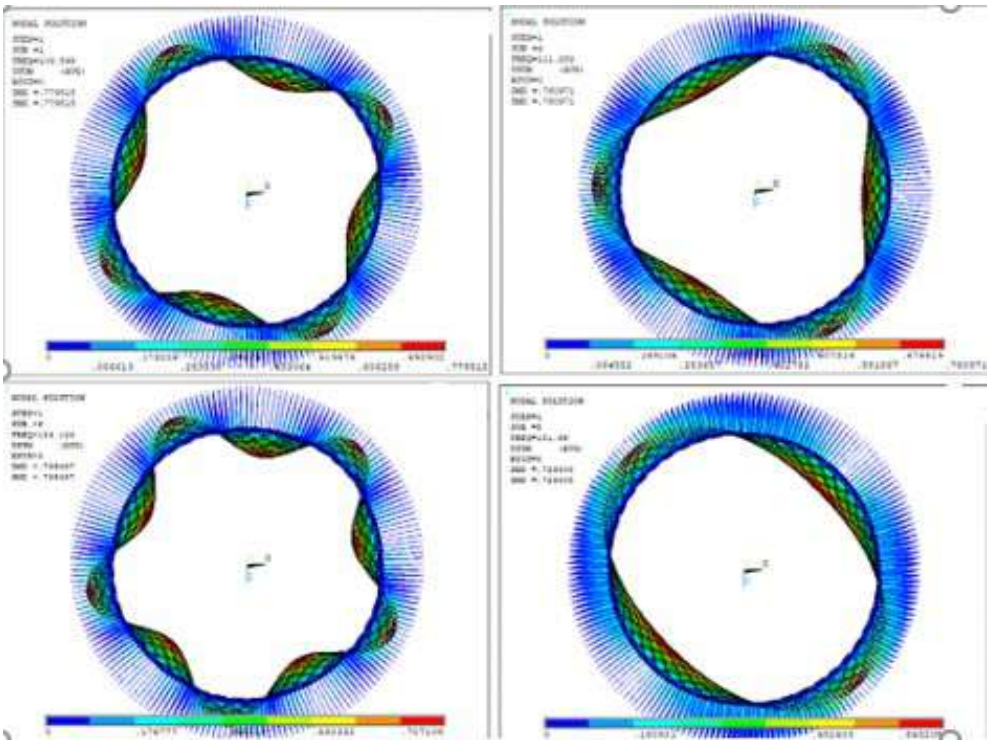

Figure 9: First, third, fifth and seventh mode shapes.

effect on fundamental frequency is shown in Table 4. The natural frequencies derived from analytical solution and FEM are compared in Table 4 for $n_s = 48$ ribs and the error values are also calculated. These calculations could be performed for $n_s = 60$ and 72 ribs vs other angles which leads to many diagrams. The trend of increasing the fundamental frequency can be compared between two sets of results in the same table and is shown as

Table 3: Natural frequencies calculated by analytical formula varying elastic foundation coefficients for $L = 2$m.

(K,G)	Natural Frequency (Hz)	(K,G)	Natural Frequency (Hz)	(K,G)	Natural Frequency (Hz)	(K,G)	Natural Frequency (Hz)
(10 , 0)	100.86	(10 , 10)	100.92	(10 , 25)	101.02	(10 , 50)	101.19
(100 , 0)	100.86	(100 , 10)	100.93	(100 , 25)	101.03	(100 , 50)	101.19
$(2\times10^3,0)$	100.89	(1000 , 10)	100.95	(1000 , 25)	101.05	(1000 , 50)	101.21
$(10^4,0)$	101.10	$(10^4$, 10)	101.17	$(10^4,25)$	101.27	$(10^4,50)$	101.44
$(10^5,0)$	103.30	$(10^5,10)$	103.37	$(10^5,25)$	103.47	$(10^5,50)$	103.63
$(10^6,0)$	123.17	$(10^6,10)$	123.22	$(10^6,25)$	123.30	$(10^6,50)$	123.481
$(2\times10^6,0)$	142.01	$(2\times10^6,10)$	142.06	$(2\times10^6,25)$	142.13	$(2\times10^6,50)$	142.25
$(3\times10^6,0)$	158.63	$(3\times10^3,10)$	158.67	$(3\times10^6,25)$	158.74	$(3\times10^6,50)$	158.84
(K,G)	Natural Frequency (Hz)	(K,G)	Natural Frequency (Hz)	(K,G)	Natural Frequency (Hz)	(K,G)	Natural Frequency (Hz)
(10,75)	101.35	(10,100)	101.52	(10,500)	104.13	(10,1000)	107.30
(100,75)	101.36	(100,100)	101.52	(100,500)	104.13	(100,1000)	107.31
(1000,75)	101.38	(1000,100)	101.54	(1000,500)	104.15	(1000,1000)	107.32
$(10^4,75)$	101.601	$(10^4,100)$	101.77	$(10^4,500)$	104.37	$(10^4,100)$	107.531
$(10^5,75)$	103.79	$(10^5,100)$	103.95	$(10^5,500)$	106.50	$(10^5,1000)$	109.60
$(10^6,75)$	123.57	$(10^6,100)$	123.71	$(10^6,500)$	125.86	$(10^6,1000)$	128.49
$(2\times10^6,75)$	142.36	$(2\times10^6,100)$	142.48	(10,500)	104.13	$(2\times10^6,103)$	146.65
$(3\times10^6,75)$	158.95	$(3\times10^6,100)$	159.05	(100,500)	104.13	$(3\times10^6,103)$	162.80

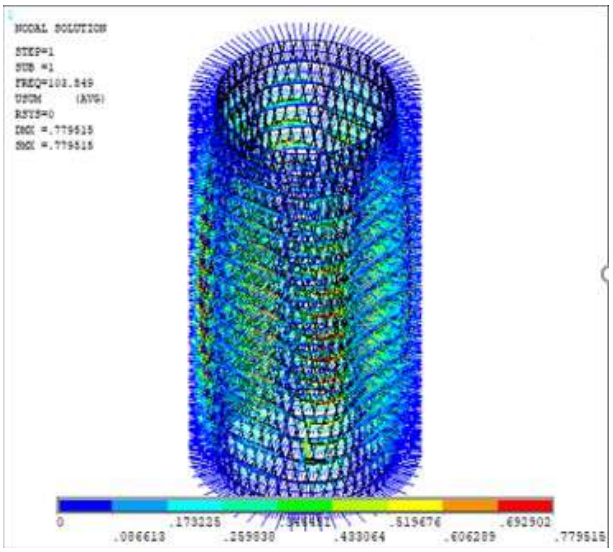

Figure 10: The first mode shape of lattice cylindrical shell in elastic ambient.

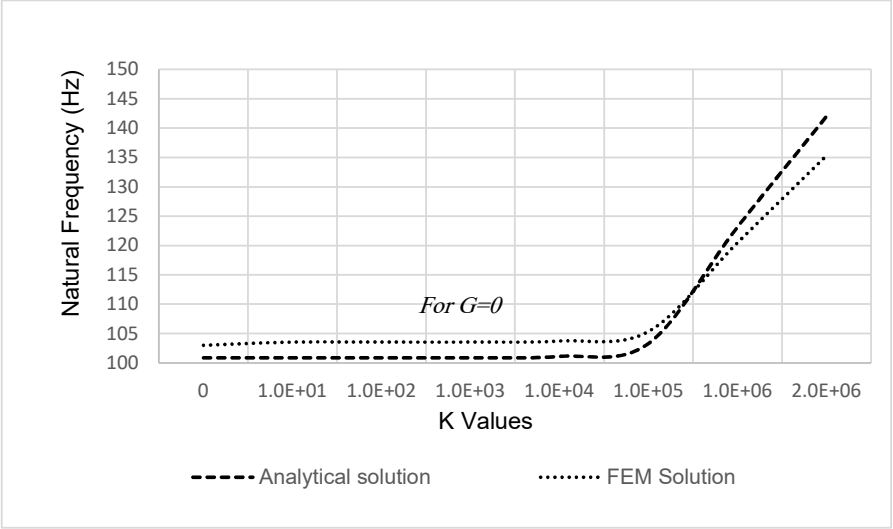

Figure 11: Comparison of analytical and FEM solutions vs Winkler coefficient.

a graph in Fig. 11. In Table 4, the natural frequencies from analytical formula and FEM solutions are compared for different Winkler coefficients and the acceptable error values show a good agreement between the two methods. Also it is observed that by increasing the Winkler coefficient of the foundation, the natural frequencies will increase.

Table 4: Changes of natural frequencies due to foundation winkler coefficient variations for $n_s = 48$.

(K,G)	Analytical solution/ Natural Frequencies	FEM Solution of Natural Frequencies	Error%
(0,0)	100.86	103.01	2.13
(10,0)	100.86	103.55	2.67
$(10^2,0)$	100.86	103.55	2.67
$(10^3,0)$	100.88	103.55	2.65
$(10^4,0)$	101.11	103.73	2.60
$(10^5,0)$	103.31	105.37	2.00
$(10^6,0)$	123.17	120.49	2.17
$(2\times10^6,0)$	142.01	135.33	4.70

5 Conclusions

A free vibration problem of composite lattice circular cylindrical shell, surrounded by Winkler–Pasternak ambient, with clamped ends has been solved. Continuous model has been replaced with the lattice structure, assuming equivalent effective orthotropic stiffness characteristics. The analytical formulation has been solved analytically, using both Fourier decomposition and the Galerkin method. The integrated formula was solved for natural frequencies of lattice shell enclosed in an elastic ambient. The results were verified using the Finite-Element Method. For FEM simulations, the coefficients of Winkler and Pasternak characteristics, were replaced by shear and radial springs, respectively. The fundamental frequency of the system is dependent on elastic foundation characteristics, thus the variation of radial and shear springs stiffness, cause different natural frequencies. It was observed that by increasing the springs stiffness, more system stability can be expected. Application of both analytical and numerical methods, demonstrated that higher values for the system structural parameters are needed for a system with shortened length. The efficiency of the analytical formula has been confirmed using FEM numerical calculations. This parametric formula enables efficient assessment of the appropriateness of both radial and shear springs stiffness in the design analysis.

Appendix

$$A_{11}=2E_S\frac{\delta_S}{a_s}\cos^4\phi,\quad A_{12}=A_{33}=2E_S\frac{\sigma_S}{a_s}\cos^2\phi\sin^2\phi,\quad A_{22}=2E_S\frac{\sigma_s}{a_s}\sin^4\phi+E_r\frac{\sigma_r}{a_r},$$

$$A_\rho=2\rho_s\frac{\delta_s}{a_s}+\rho_r\frac{\delta_r}{a_r},\quad B_{11}=A_{11}h, B_{12}=A_{12}h,\quad B_{22}=A_{22}h,\quad B_{33}=A_{33}h,\quad B_p=A_\rho h,$$

$$D_{11}=A_{11}\frac{h^3}{12},\quad D_{12}=A_{12}\frac{h^3}{12},\quad D_{22}=A_{22}\frac{h3}{12},\quad D_{33}=A_{33}\frac{h^3}{12},$$

$$c_{11}=a_1a_{32}-{a_{12}}^2,\quad c_{12}=c_{21}=a_{11}a_{23}-a_{12}a_{13},\quad c_{22}=a_{11}a_{33}-a_{13}^2,\quad g_{11}=e_{22}a_{11},$$

$$g_{22}=a_{11}e_{33},\quad P_{ss}=a_{11}P_s,\quad P_S=\frac{t}{E_s\sigma_s n_s}\left[G\frac{\xi}{S}+\left(K\frac{R^2}{L^2}+\frac{Gn^2}{L^2}\right)s\right],$$

$$a_{11}=f_{11}\frac{\lambda^4}{s}+f_{12}\xi sn^2,\quad a_{12}=a_{21}=2f_{12}\xi n,\quad a_{31}=a_{13}=f_{12}\xi,\quad a_{12}=(1+Z)\left(f_{12}\frac{\xi}{s}+f_{22}sn^2\right),$$

$$a_{23}=a_{32}=n\left[f_{22}\left(1+zn^2\right)s+3f_{12}z\frac{\xi}{s}\right],\quad a_{33}=\left[f_{11}z\frac{\lambda^4}{s^4}+f_{22}\left(1+zn^4\right)\right]s+6f_{12}zn^2\frac{\xi}{s},$$

$$a_{22}=(1+Z)\left(f_{12}\frac{\xi}{s}+f_{22}sn^2\right),\quad e_{11}=f_\rho\xi,\quad e_{22}=e_{33}=f_\rho,\quad z=\frac{1}{12t^2},\quad t=\frac{R}{h}.$$

References

[1] T. WANG, AND J. STEPHENS, *Natural frequencies of timoshenko beams on pasternak foundations,* J. Sound Vib., 51(2) (1977), pp. 149–155.

[2] A. KHALIFA, *Natural frequencies and mode shapes of variable thickness elastic cylindrical shells resting on a pasternak foundation,* J. Vib. Control, 17(8) (2016), pp. 1158–1172.

[3] D. PALIWAL AND R. PANDEY, *Free vibrations of an orthotropic thin cylindrical shell on a pasternak foundation,* AIAA J., 39(11) (2001).

[4] A. LOPATIN, E. MOROZOV AND A. SHAATOV, *An analytical expression for fundamental frequency of the composite lattice cylindrical shell with clamped edges,* J. Compos. Struct., 141 (2016), pp. 232–239.

[5] A. LOPATIN, E. MOROZOV AND A. SHAATOV, *Fundamental frequency of a cantilever composite filament-wound anisogrid lattice cylindrical shell,* J. Compos. Struct., 133 (2015), pp. 564–575.

[6] V. VASILIEV AND V. BRAYAN, *Anisogrid composite lattice structures-development and aerospace applications,* J. Compos. Struct., 94(3) (2012), pp. 1117–1127.

[7] V. VASILIEV, V. BRAYAN AND A. RASIN, *Anisogrid lattice structures-survey of development and application,* J. Compos. Struct., 54(2–3) (2001), pp. 361–370.

[8] A. HOU AND K. GRAMOLL, *Compressive strength of composite lattice structures,* J. Reinforced Plastics Compos., 17(5) (1998).

[9] G. TOTARO, *Local buckling modelling of isogrid and anisogrid lattice cylindrical shells with hexagonal cells,* J. Compos. Struct., 95 (2013), pp. 403–410.

[10] M. XU AND Z. QIU, *Free vibration analysis and optimization of composite lattice truss cores and sandwich beams with interval parameters,* J. Compos. Struct., 106 (2013), pp. 85–95.

[11] E. FRULLONI, P. CONTI AND L. TORRE, *Experimental study and finite element analysis of the elastic instability of composite lattice structures for aeronautic applications,* J. Compos. Struct., 78 (2007), pp. 519–528.

[12] M. JEON, S. KONG, I. KIM AND S. LEE, *Failure load prediction of anisogrid cylindrical composite lattice structures using failure criterion based on ratio of bending to compressive stress,* J. Mech. Sci. Tech., 35 (2021), pp. 4897–4906.

[13] Y. KIM, P. KIM, H. KIM AND J. PARK, *Optimal design of a composite lattice rectangular plate for solar panels of a high-agility satellite,* Int. J. Aeron. Space Sci., 19 (2018), pp. 762–775.